ELSEVIER

www.elsevier.nl/locate/jorganchem

Journal of Organometallic Chemistry 596 (2000) 212–220

Journal of Organometallic Chemistry

Density functional calculations of dinuclear organometallic carbonyl complexes. Part I: metal–metal and metal–CO bond energies

Timothy A. Barckholtz [1], Bruce E. Bursten *

Department of Chemistry, The Ohio State University, Columbus, OH 43210-0440, USA

Received 9 August 1999; received in revised form 5 November 1999

Dedicated to Professor F. Albert Cotton, friend, colleague, mentor, and pioneer of metal–metal bonding, on the occasion of his 70th birthday.

Abstract

One of the most fundamental properties in chemistry is the bond dissociation energy (BDE), the energy required to break a specific bond of a molecule. In this paper we apply gradient-corrected density functional theory (DFT) to the calculation of the BDEs of three prototypical organometallic complexes, $Mn_2(CO)_{10}$, $Fe_2(CO)_9$, and $Co_2(CO)_8$, along with the CO-loss products $Mn_2(CO)_9$ and $Mn_2(CO)_8$. We consider the dissociation of both the metal–metal bond and a metal–carbonyl bond. For $Mn_2(CO)_{10}$ and $Fe_2(CO)_9$, the calculated metal–metal BDE is within the error of the experimental measurements. However, the calculated metal–metal BDE for $Co_2(CO)_8$ is not within the errors of the measurements, but is improved greatly with an unrestricted wavefunction compared with a restricted wavefunction. For the first carbonyl BDE, the calculations agree within a few kcal mol^{-1} for each complex.

Keywords: Metal carbonyls; Bond energies; Density functional theory

1. Introduction

In the last few years, density functional theory (DFT) has become a very popular computational method for the calculation of a number of molecular properties [1–4]. For many years the accuracy of these calculations lagged behind that of traditional methods based on Hartree–Fock calculations. However, the development of non-local (or gradient-corrected) functionals has closed the gap, and in many instances DFT leads to a greater agreement with experiment than do Hartree–Fock methods for a variety of molecular properties. Because of its greater computational efficiency, in terms of the quality, with respect to computational expense, DFT has been applied extensively to inorganic and organometallic complexes [5].

One area that has yet to be fully explored is the application of DFT to cluster complexes, of which the simplest type are molecules with only two transition metals. While DFT has performed very well with respect to the calculation of molecular properties of mononuclear complexes [6–31], the application of these calculations to complexes with metal–metal bonds has been much less studied [32–40]. Similarly, few calculations have been reported on complexes that may not have a direct metal–metal bond, but where the two transition metals are linked by bridging and/or semi-bridging carbonyl ligands.

In two other papers [41,42], we have shown that non-local DFT calculates the geometries of dinuclear organometallic complexes (DOCs) with a high degree of accuracy, performing especially well with respect to the metal–metal bond lengths. Additionally, these calculations showed that the relative energies of different isomers of a given complex are reasonably well reproduced, and that the vibrational frequencies of the C–O

* Corresponding author.

[1] Present address: JILA, University of Colorado, Boulder, CO 80309-0440, USA.

0022-328X/00/$ - see front matter
PII: S0022-328X(99)00696-8

stretching motions and the metal–metal stretch are also calculated accurately. Indeed, nonlocal DFT has provided results so accurate that it can be used as a structural probe for molecules that are too fragile to characterize by usual experimental techniques. For example, we have used these calculations to determine the structures, based on comparisons of calculated and experimental infrared spectra, of the unstable photochemical CO-loss products of $Mn_2(CO)_{10}$ [43] and $Cp_2Fe_2(CO)_4$ ($Cp = \eta^5$-C_5H_5) [44]. These calculations can also be used to assess the metal–metal bonding in these clusters [43].

In this paper, we apply nonlocal DFT methodology to the calculation of metal–metal and metal–carbonyl bond energies for the dinuclear complexes $Mn_2(CO)_{10}$ (**1**), $Fe_2(CO)_9$ (**2**), $Co_2(CO)_8$ (**3**), $Mn_2(CO)_9$ (**4**), and $Mn_2(CO)_8$ (**5**). Bond dissociation energies (BDEs) are cornerstones in the thermochemistry of molecular systems, and their experimental determination for organometallic complexes remains a difficult task [45,46]. While a number of workers have reported calculations of BDEs of mononuclear organometallic complexes [21–31], to our knowledge the only calculations reported for metal–metal BDEs are those of Folga and Ziegler [33] for $Mn_2(CO)_{10}$ and $Co_2(CO)_8$. It is the purpose of this paper to address more fully the DFT calculation of metal–metal and metal–carbonyl BDEs. We present in detail only the calculations of the mononuclear fragments, since the geometries and vibrational frequencies of all of the dinuclear organometallic complexes have been fully reported elsewhere [41–43].

2. Computational details

The density functional calculations were performed with the Amsterdam Density Functional (ADF) program version 2.1 (Theoretical Chemistry, Vrije Universiteit, Amsterdam, The Netherlands), developed by Baerends et al. [47–49]. The frozen core approximation was applied to the innermost orbitals of all atoms: [1s] for C and O and [1s–2p] for the transition metals. The STO valence basis set used for the C and O atoms was a double-ζ plus a 3d-type polarization functions, which comprises the III basis set of ADF. The STO valence basis set for the transition metals was triple-ζ for the metal nd and $(n+1)$s orbitals and single-ζ for the $(n+1)$p orbital (the IV basis set of ADF).

The functionals used in the calculations were the local density approximation of Vosko et al. [50] combined with the gradient corrections for the exchange of Becke [51] and for the correlation of Perdew [52] (BP). The geometries were optimized to a maximum gradient of less than 0.0001 hartree $Å^{-1}$. The frequency calculations were performed using two-sided numerical differentiation of the Cartesian coordinates with a step size of 0.01 Å. The calculated frequencies for the mononuclear fragments have been shifted by $+17$ cm^{-1}, as discussed elsewhere [41].

For those molecules that contained open-shell ground states, calculations were performed using both the restricted and unrestricted spin density formalisms. For some fragments, the HOMO was degenerate and partially occupied. (For example, the HOMO of $Mn(CO)_3$ is an e orbital with only one electron.) In these cases, the electrons were distributed equally amongst the orbitals. This formalism results in fractional occupations of each orbital, which is completely allowed within the density functional formalism. This approach results in the calculation of the average electron density for the possible states derived from the open-shell configuration.

3. Results

Our focus in this paper is the calculation of two important BDEs for DOCs, namely the metal–metal and metal–carbonyl BDEs. We shall calculate the bond energies for only the equilibrium reactants and products, which corresponds to what is measured in most experiments. The calculation of these quantities requires the optimized geometries and total energies of both the reactants and products of the bond-breaking reaction. Others [33] have considered a bond snapping enthalpy, which is a theoretical quantity for the energy released upon breaking the bond without complete relaxation of the geometries, and perhaps electronic excited states, of the nascent fragments.

3.1. Mononuclear fragment complexes

The metal–metal BDE of a dinuclear complex corresponds to the total energy difference between the dinuclear complex and two mononuclear fragments, which are assumed to relax to their equilibrium geometries after metal–metal bond scission. Thus, the calculation of the metal–metal BDE requires that the optimized geometries and energies of the mononuclear fragments be calculated. These calculations are often complicated somewhat by the fact that many of the fragments are necessarily open-shell systems. We have used both restricted and unrestricted wavefunctions for the open-shell molecules, and we shall compare the two sets of results. Many authors have previously considered the structures of a number of these mononuclear fragments, but using slightly different functionals or basis sets [24–29,53–57]. We shall present our results only briefly, as they do not differ substantially from these previous works. Where possible, we have verified the accuracy of the calculations by comparisons of the calculated and experimental C–O stretching frequencies.

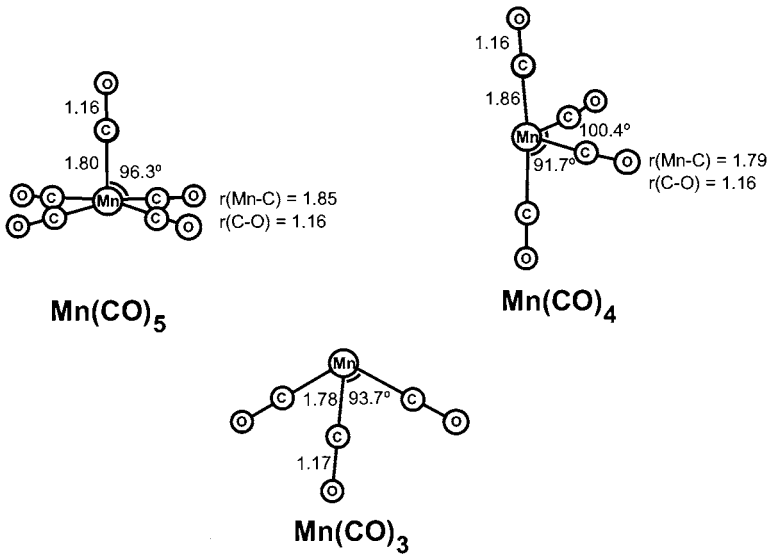

Fig. 1. Optimized geometries, at the BP level, of $Mn(CO)_5$, $Mn(CO)_4$, and $Mn(CO)_3$.

For the three Mn complexes, the possible mononuclear fragments are $Mn(CO)_5$, $Mn(CO)_4$, and $Mn(CO)_3$; it is noteworthy that we have proposed an isomer of the double-CO loss photoproduct **5** that has an unusual asymmetric $(OC)_5Mn–Mn(CO)_3$ ligand distribution [41,42]. The optimized geometries of these three $Mn(CO)_n$ species are shown in Fig. 1. As is well established [58,59], the geometry of $Mn(CO)_5$ is square pyramidal, with a $^2A_1$ ground state under the C_{4v} point group. The calculations lead us to propose that the 15-electron complex $Mn(CO)_4$ has a C_{2v} geometry with a $^2B_1$ ground state, while the 13-electron complex $Mn(CO)_3$ is of C_{3v} symmetry with a ^2E ground state. The calculated C–O stretching vibrational frequencies, along with the available experimental data for $Mn(CO)_5$ [58], are presented in Table 1 for all three $Mn(CO)_n$ complexes. As expected, there is excellent agreement between the calculated and observed C–O stretching frequencies for $Mn(CO)_5$.

Breaking $Fe_2(CO)_9$ (**2**) into mononuclear fragments is a more complicated process than the homolysis of $Mn_2(CO)_{10}$ because of (a) the presence of bridging ligands; and (b) the odd number of CO ligands. It is not unreasonable to assume that **2** would dissociate into an $Fe(CO)_5$ fragment, which is a stable molecule in its own right, and $Fe(CO)_4$, an unstable 16-electron complex, first characterized experimentally by Poliakoff and Turner [60]. Fig. 2 illustrates the optimized geometries for these two $Fe(CO)_n$ complexes. While $Fe(CO)_5$ clearly possesses a singlet ground state, the geometry and spin state of the ground state of $Fe(CO)_4$ has been the subject of a large number of calculations [24–29,53–55], which have eventually led to the general agreement that the triplet is a few kcal mol^{-1} lower in energy than the singlet. We calculate the two isomers to

Table 1
Calculated and experimental C–O stretching frequencies (cm^{-1}) for $Mn(CO)_5$, $Mn(CO)_4$, and $Mn(CO)_3$

Molecule	Symmetry	Calculated ν_{CO} [a]	Experimental ν_{CO} [b]
$Mn(CO)_5$ (C_{4v})	a_1	2092 (2094)	2105 [c]
	b_2	2004 (2009)	2018 [c]
	a_1	1992 (1993)	1978
	e	1990 (1993)	1988
$Mn(CO)_4$ (C_{2v})	a_1	2062 (2065)	
	a_1	1965 (1971)	
	b_2	1965 (1967)	
	b_1	1947 (1948)	
$Mn(CO)_3$ (C_{3v})	a_1	2005 (2005)	
	e	1916 (1904)	

[a] Values in parentheses are from the unrestricted calculations.
[b] Experimental values from Refs. [58,59].
[c] Value obtained from a force field calculation based on the experimental data.

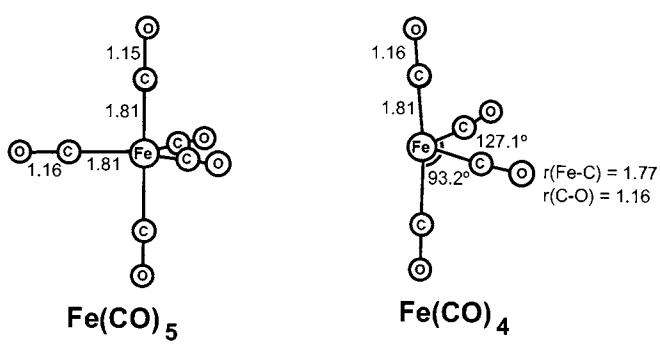

Fig. 2. Optimized geometries, at the BP level, of $Fe(CO)_5$ and $Fe(CO)_4$.

Table 2
Calculated and experimental C–O stretching frequencies (cm^{-1}) for $Fe(CO)_5$ and $Fe(CO)_4$ [a]

Molecule	Symmetry	Calculated ν_{CO}		Experimental ν_{CO} [b]
$Fe(CO)_5$ (D_{3h})	a_1'	2112		2116
	a_1''	2027		2030
	a_2'	2023		2028
	e_1'	2009		1989
		$^1A_1$	$^3B_2$	
$Fe(CO)_4$ (C_{2v})	a_1	2085 (87)	2071 (0)	2088 (1)
	a_1	1990 (100)	1998 (42)	1999 (100)
	b_2	1989 (27)	1990 (100)	1994 (33)
	b_1	1968 (0)	1987 (57)	1975 (22)

[a] For $Fe(CO)_4$, the calculated absolute intensities and experimental relative intensities are given in parentheses for a better comparison between the calculated and experimental values.
[b] Experimental values from Refs. [60,88].

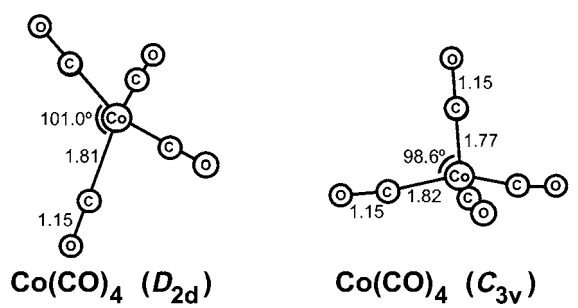

Fig. 3. Optimized geometries, at the BP level, of $Co(CO)_4$.

Table 3
Calculated and experimental C–O stretching frequencies (cm^{-1}) for $Co(CO)_4$

Molecule	Symmetry	Calculated ν_{CO} [a]	Experimental ν_{CO} [b]
$Co(CO)_4$ (D_{2d})	a_1	2085 (2084)	
	b_2	2003 (2004)	
	e	2001 (2003)	
$Co(CO)_4$ (C_{3v})	a_1	2092 (2092)	2107
	a_1	2024 (2019)	2029
	e	2019 (2016)	2011

[a] Values in parentheses are from the unrestricted calculations.
[b] Experimental values from Ref. [61].

be nearly isoenergetic, with the singlet being more stable by only 0.02 kcal mol^{-1}. As can be seen in Table 2, the calculated C–O stretching frequencies for the triplet state agree quite well with the experimental values.

Both the bridged and unbridged isomers of $Co_2(CO)_8$ (**3**) are expected to dissociate into two 17-electron $Co(CO)_4$ fragments. The best experimental data on the $Co(CO)_4$ radical is from the work of Hanlan et al. [61], who obtained the infrared and ESR spectra of $Co(CO)_4$ in rare gas matrices. The radical has also been the subject of previous theoretical calculations [56,57], which predict that the C_{3v} and D_{2d} isomers are very close in energy. Our calculations show that the D_{2d} isomer is lower in energy than the C_{3v} isomer by only 1 kcal mol^{-1} (Fig. 3). To determine which isomer is actually observed, the calculated and experimentally observed C–O stretching frequencies for these two isomers of this fragment are given in Table 3. There is a slightly better agreement between the experimental frequencies and those calculated for the C_{3v} isomer, and we therefore propose that the experimentally observed isomer is of C_{3v} symmetry.

For the organometallic radicals $Mn(CO)_5$, $Mn(CO)_4$, $Mn(CO)_3$, and $Co(CO)_4$, we calculated the geometries, frequencies, and energies using both restricted and unrestricted wavefunctions. The geometries of the two methods are virtually identical, with the bond lengths varying by less than 0.1 Å. While the frequencies were different between the two methods (see Tables 1 and 3), these differences are not large enough to be very significant. However, the calculated energies were quite different, with the unrestricted wavefunctions being several kcal mol^{-1} lower in energy. This added stabilization of the unrestricted wavefunctions has a significant effect on the calculated metal–metal bond energies, which are discussed in Section 4.1.

3.2. Dinuclear complexes

We have reported elsewhere the optimized geometries and vibrational frequencies [41–43] for all of the dinuclear carbonyl complexes discussed here, except for $Fe_2(CO)_8$. For the geometry of $Fe_2(CO)_8$, we have reproduced the lowest-energy structure found by Jacobsen and Ziegler [37]. Fig. 4 presents the structures of all of the dinuclear complexes required to calculate the CO BDEs of interest. For $Mn_2(CO)_8$ and $Co_2(CO)_8$, we show the structures of two isomers for each; we discuss the relative energies of these isomers in Section 4.1 in relation to the metal–metal bond strengths of these isomers. Elsewhere [41], we have considered a third isomer of $Co_2(CO)_8$, which is nearly isoenergetic to the two shown in Fig. 4, but is not considered further in this work. We optimized the structure of $Co_2(CO)_7$ to that shown in Fig. 4.

3.3. CO

In order to calculate the metal–carbonyl BDEs, we require the energy of the free CO molecule. Our BP calculations on CO led to an C–O bond length of 1.14 Å, which compares reasonably well with the experimen-

tal value of 1.13 Å for free CO in the gas phase [62]. The calculated value for the vibrational frequency is 2141 cm^{-1}, only 29 cm^{-1} lower than the gas phase value for ω_e [62].

4. Discussion

In all of our calculations of the BDEs, the product fragments are fully optimized to their lowest-energy structure. While we have shown that our calculations are accurate with respect to the vibrational frequencies of the C–O and M–M stretching modes [41], we have not assessed their accuracy for the multitude of low-frequency modes that arise from the metal–ligand stretching, bending, and torsional motions. For this reason, we do not include the zero-point energy of the molecules in the calculation of the BDEs. We feel that this omission will not add significantly to the error of the calculations; the corrections due to the metal–metal and metal–ligand stretching frequencies (corresponding to the bonds being broken) are small compared with the overall BDEs of these complexes. In addition, we do not make any temperature, pressure, or other corrections to the calculated dissociation energy. As a result, our calculations of the BDEs correspond to ΔE_e for the bond dissociation, whereas the experiments measure ΔH_0. We expect that the errors introduced by these approximations are insignificant relative to the overall errors in the calculations (and experiments) themselves.

4.1. M–M bond dissociation energies

For those DOCs that do not contain bridging ligands, such as $Mn_2(CO)_{10}$ (**1**), the dissociation energy of the metal–metal bond should be a direct reflection of the strength of the metal–metal bonding in the system. Thus, the M–M BDE of **1** corresponds to the energy needed to break the unambiguous Mn–Mn bond, forming two relaxed $Mn(CO)_5$ radicals:

$$(OC)_5Mn–Mn(CO)_5 \rightarrow (OC)_5Mn^{\bullet} + {}^{\bullet}Mn(CO)_5 \quad (1)$$

For those complexes that contain bridging carbonyl ligands, such as **2** and the bridged form of **3**, the interpretation of the metal–metal BDE is more compli-

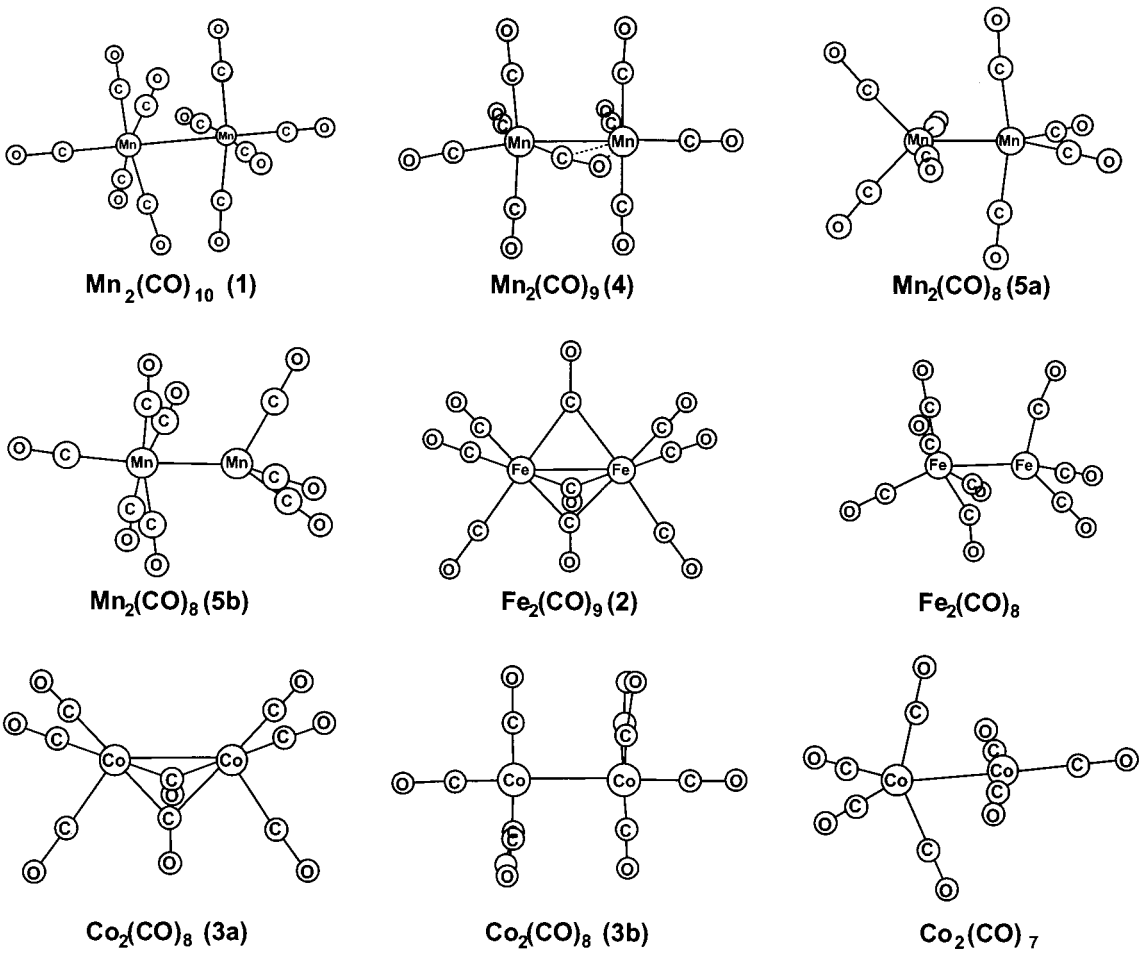

Fig. 4. Optimized geometries, at the BP level, of the DOCs relevant to the calculation of the M–CO bond dissociation energies of interest.

Table 4
Calculated M–M and M–CO bond dissociation energies (kcal mol^{-1}) for the DOCs [a]

Molecule	M–M BDE		First M–CO BDE	
	Calculated [b]	Experimental	Calculated	Experimental
$Mn_2(CO)_{10}$ (**1**)	45.5 (38.9)	38	35.5	38
$Fe_2(CO)_9$ (**2**)	29.5 [c]	29	32.3	28
$Co_2(CO)_8$ (C_{2v}; **3a**)	45.8 (34.9)	19	31	32
$Co_2(CO)_8$ (D_{3d}; **3b**)	40.8 (29.9)		26	
$Mn_2(CO)_9$ (**4**)	54.1 (46.3)		35.9	
$Mn_2(CO)_8$ (**5a**)	62.4 (53.3)			
$Mn_2(CO)_8$ (**5b**)	61.0 (54.0) [d]			

[a] See text for references to experimental values.
[b] Values in parentheses are from the unrestricted calculations.
[c] Calculated for the dissociation into $Fe(CO)_5$ and $Fe(CO)_4$ fragments.
[d] Calculated for the dissociation into $Mn(CO)_5$ and $Mn(CO)_3$ fragments.

cated. For these molecules, the notion of an M–M BDE is somewhat of a misnomer inasmuch as the energy difference between the DOC and its mononuclear fragments will contain significant contributions from the M-(μ-CO) bonds. The M–M BDE values that we report for these molecules are simply the energies needed for fragmentation, without an attempt to sort out the M–M and M–(μ-CO) contributions. In Table 4 we list the calculated M–M BDE and the first carbonyl BDE.

As noted above, $Mn_2(CO)_{10}$ has an indisputable Mn–Mn bond and homolysis of this bond leads to two identical $Mn(CO)_5$ radicals (Eq. (1)). In addition, the geometry of the $Mn(CO)_5$ moiety changes very little from $Mn_2(CO)_{10}$ to the $Mn(CO)_5$ radical, so there is minimal contribution to the Mn–Mn BDE due to fragment relaxation. Experimental measurements of its Mn–Mn bond energy vary wildly, from 19 to 42 kcal mol^{-1}, with the most recent measurements converging on a value of 38 ± 5 kcal mol^{-1} [45,63,64]. Our calculated values of the M–M bond energy in **1** are 45.5 kcal mol^{-1} (restricted) and 38.9 kcal mol^{-1} (unrestricted), in reasonable agreement with the experiments, especially when the scatter in the experimental measurements is considered. Our value is also very close to the value of 41.6 kcal mol^{-1} calculated by Folga and Ziegler [33] using very similar methodology.

Photochemical studies of **1** by others [65,66] and by us [67] have led to the formation of the unsaturated CO-loss products **4** and **5**. The loss of CO ligands is accompanied by a formal increase in the Mn–Mn bond order. Molecule **4** contains a semi-bridging CO that, in principle, can act as a four-electron donor. Nevertheless, the Mn–Mn bond in **4** is expected to have an order between one and two. Molecule **5a** is a symmetric DOC with only terminal CO ligands. It therefore has a formal Mn–Mn triple bond. As shown in Table 4, the Mn–Mn BDEs follow the order $\mathbf{1} < \mathbf{4} < \mathbf{5}$, in accordance with these bond order considerations. The asymmetric isomer **5b** is calculated to be 2.8 kcal mol^{-1} higher in energy than isomer **5a**, which implies a Mn–Mn bond that is approximately 2.8 kcal mol^{-1} weaker in **5b** than in **5a**, assuming the other geometric changes have no effect on the thermochemistry.

For **2**, our calculated value of the Fe–Fe BDE corresponds to the energy difference for the dissociation of the molecule into $Fe(CO)_5$ and $Fe(CO)_4$:

$$Fe_2(CO)_9 \rightarrow Fe(CO)_5 + Fe(CO)_4 \quad (2)$$

This calculation is not a direct measurement of the metal–metal bond strength, because of the contributions of bridging carbonyl ligands. Nevertheless, the energy difference in Eq. (2) does correspond to the experimental measurements of the Fe–Fe bond energy, thus allowing a meaningful comparison between our calculated value and the available experimental data. Two experimental measurements have been reported for this bond energy and, as with the Mn–Mn bond energy in **1**, the measurements do not agree with one another: Connor reports a BDE of 9 kcal mol^{-1} for **2** [68] while Baev has estimated it to be 29 kcal mol^{-1} [69]. Our calculated value of 29.5 kcal mol^{-1} is clearly more consistent with the latter measurement.

The observation that the M–M BDE for **1** is significantly greater than that of **2** is interesting and, at first glance, nonintuitive. Complex **1** has only a single Mn–Mn bond holding the two $Mn(CO)_5$ fragments together whereas **2** has the Fe–Fe bond and three Fe–(μ-CO)–Fe bonds that must be broken in the dissociation reaction of Eq. (2). The total energy of the fragment products of Eq. (2) are lowered by two factors in the process: (1) the formation of terminal M–CO bonds from what were previously bridging bonds; and (2) the geometric reorganization of the $Fe(CO)_5$ and $Fe(CO)_4$ fragments. From studies of the fluxionality of first-row transition metals, it is well known that the energy difference between two terminal carbonyl ligands and two bridging carbonyl ligands is very small, i.e. the following generic reaction is nearly thermoneutral [70]:

$$OC–M–M–CO \rightarrow M_2(\mu\text{-}CO)_2 \quad (3)$$

This energetic equivalence of terminal and bridging carbonyls suggests that bridging carbonyls should not significantly contribute to the value of the BDE; thus, the M–M BDE in systems with bridging carbonyls will be dominated by the M–M contribution. Under this assumption, the calculated and experimental M–M BDE values in Table 4 therefore imply that the Mn–Mn bond in **1** is 9–16 kcal mol^{-1} stronger than the Fe–Fe bond in **2**.

The situation with respect to the M–M BDE of $Co_2(CO)_8$ is interesting from two respects, namely its low experimental value and the difference between the calculated values upon using restricted and unrestricted wavefunctions for $Co(CO)_4$. The dimer $Co_2(CO)_8$ exists in two dominant forms: a C_{2v} form with two bridging CO ligands (**3a**) and an all-terminal form of D_{3d} symmetry (**3b**). Isomer **3a** is slightly lower in energy than **3b** and hence is the dominant form of the molecule in solution and in the gas phase. Our calculations place **3b** ca. 5.0 kcal mol^{-1} higher in energy than **3a**, which is consistent with the available experimental estimates of the energy difference [71–76]. A third isomer, of D_{2d} symmetry, is also low in energy, but has only been observed in low-temperature matrices.

The dissociation of $Co_2(CO)_8$ is assumed to lead to the same products; two equivalent and relaxed $Co(CO)_4$ fragments, for both **3a** and **3b**:

$$Co_2(CO)_8 \text{ (}\mathbf{3a}\text{ or }\mathbf{3b}\text{)} \rightarrow 2Co(CO)_4 \quad (4)$$

Because the BDE is the energy difference for the above reaction, the calculated BDE for **3b**, 29.9 kcal mol^{-1} (unrestricted), is smaller than that of **3a**, 34.9 kcal mol^{-1} (unrestricted), by precisely the difference in the total energies of the two isomers. The small difference between the BDEs of **3a** and **3b** reinforces the discussion above regarding the small contribution of bridging CO ligands to the M–M BDE values. Our value for **3a** is also very close to the value of 35.4 kcal mol^{-1} calculated by Folga and Ziegler [33] using very similar methodology.

The experimental measurements for the Co–Co BDE of **3** are lower than the calculated values using both the restricted and unrestricted wavefunctions, although the unrestricted calculation is significantly closer. Armentrout and co-workers recently used mass spectrometry to measure the Co–Co BDE in **3** in the gas phase and obtained a value of 20 ± 7 kcal mol^{-1} [77]. Other measurements of this bond energy vary from 15 to 22 kcal mol^{-1} [45,68,78–80]. An additional measurement of the Co–Co bond strength comes from a solution NMR study [81] of the magnetic susceptibility of the equilibrium between $Co_2(CO)_8$ and $Co(CO)_4$. The Co–Co BDE obtained in this way was 19 ± 2 kcal mol^{-1}, in excellent agreement with the gas-phase measurement of Armentrout and co-workers. The calculations of the BDE for $Co_2(CO)_8$ illustrate most vividly the necessity of using unrestricted wavefunctions for the open-shell fragments to obtain accurate BDEs.

To investigate the discrepancy between the calculated and experimental values of the BDE of $Co_2(CO)_8$, we consider whether the total energy of $Co_2(CO)_8$ is calculated too low or the total energy of $Co(CO)_4$ is calculated too high. The accurate calculation of the CO BDE in $Co_2(CO)_8$ (vida supra) indicates that the total energy calculations of $Co_2(CO)_8$, $Co_2(CO)_7$, and CO must each be accurate to within a few kcal mol^{-1}. (The alternative is that the errors fortuitously cancel, which we reject given the accuracy of the calculations of the M–CO BDEs in **1** and **2**.) The BDE of $Co_2(CO)_8$ is calculated to be 16 kcal mol^{-1} too large, which implies that the total energy of the radical is apparently 8 kcal mol^{-1} too high.

From this analysis, it would seem that the error in the calculated Co–Co BDE must lie in the calculation of the energy of the $Co(CO)_4$ radical. As a check on this discrepancy, we have calculated the BDE of the Co–H bond in $HCo(CO)_4$. The experimental values for this quantity are 54 and 59 kcal mol^{-1} [54,81], and our calculation yields a value of 70.1 kcal mol^{-1}. This comparison indicates that the calculated energy of the $Co(CO)_4$ radical is approximately 11 kcal mol^{-1} too high, which is consistent with the result obtained from the comparison of the Co–Co BDE in $Co_2(CO)_8$. We have considered a number of possible sources for this apparent discrepancy. Relativistic effects, other electronic states, lower symmetry geometries and wavefunctions, different choices of functionals, and dissociation into other fragments cannot account for the discrepancy in the bond energy calculation. At present, we are at a loss for why the density functional calculations apparently give unusually poor results for the total energy of the $Co(CO)_4$ radical.

4.2. M–CO bond energies

Our calculations of the first M–CO BDE agree well with the scant experimental measurements of them. Smith [82] has reported a BDE for $Mn_2(CO)_9$–CO of 38 kcal mol^{-1}, which is in good agreement with our calculated value of 35.5 kcal mol^{-1}. Baev measured the first CO bond energy in $Fe_2(CO)_9$ to be 27.9 kcal mol^{-1} [69], again in reasonably good agreement with our calculated value of 32.3 kcal mol^{-1}. A value of 32.2 kcal mol^{-1} was also reported [69] for the first BDE of $Co_2(CO)_8$, and our calculated value of 30.6 kcal mol^{-1} is in very good agreement with this experiment. Overall, the calculated M–CO BDEs are in reasonably good agreement with the available experimental data.

5. Conclusions

With one exception, the calculated M–M and M–CO BDEs of the dinuclear carbonyl complexes are in very good agreement with the available experimental data. Only the values calculated using the BP functional have been reported and compared with this experiment. As Becke has shown in a series of papers [83–87], the non-local functionals are far superior to local functionals for the calculation of BDEs. While Becke's calculations were done exclusively for organic molecules, similar results have been observed for organometallic complexes [21–31]. The BDEs calculated in the present study show that the non-local functionals can also be used to calculate the bond energies of both metal–metal bonds and metal–CO bonds with reasonable accuracy.

The experimental measurements for these quantities are somewhat scarce and, when available, are often in considerable disagreement with one another. It was our goal in this study to show that the use of high-quality density functional calculations could provide an additional data point that could be used to support experimental measurements. Overall, we are pleased with the agreement between our calculations and the experimental measurements, and we believe that our calculations provide support for some measurements in preference to others.

The discrepancy between our calculated value for the Co–Co BDE of $Co_2(CO)_8$ and the experimental measurements of this quantity is larger than expected. The gas-phase measurements of this bond strength rely on the combination of several different experiments, for which the presence of excited states of either the parent dimer or the fragments could affect the results. However, the thermodynamic NMR measurement in solution of the equilibrium between the dimer and the two radicals gave the same BDE as the gas-phase experiments. The agreement between these two very different means of measuring the Co–Co BDE is compelling. While the calculated BDE using an unrestricted wavefunction for $Co(CO)_4$ is significantly better than that for the restricted wavefunction, it is still larger than we would like. The accuracy of the calculated Co–CO and H–Co bond energies in $Co_2(CO)_8$ and $HCo(CO)_4$, respectively, suggests that the problem lies in a calculated energy of the $Co(CO)_4$ radical that is approximately 10 kcal mol^{-1} too high.

A final minor conclusion to be drawn from this work is the determination of the differences between results obtained using restricted and unrestricted wavefunctions. We find no significant difference between the geometries and C–O stretching vibrational frequencies using these two different formalisms. However, the energies calculated using unrestricted wavefunctions are, as expected, several kcal mol^{-1} lower than the restricted energies. Thus, we find that if only geometries and vibrational frequencies are required from the calculations, the more computationally efficient restricted calculation should be perform. If, on the other hand, a quantitative determination of the energy of the fragment is desired, the energy needs to be calculated with the unrestricted formalism.

Acknowledgements

We gratefully acknowledge support for this research from the National Science Foundation (Grant CHE-9528568), The Ohio State University, and the Ohio Supercomputer Center.

References

[1] P.C. Hohenberg, W. Kohn, L.J. Sham, Adv. Quantum Chem. 21 (1990) 7.
[2] W. Kohn, A.D. Becke, R.G. Parr, J. Phys. Chem. 100 (1996) 12974.
[3] R.G. Parr, W. Yang, Ann. Rev. Phys. Chem. 46 (1995) 701.
[4] E.J. Baerends, O.V. Gritsenko, J. Phys. Chem. A 101 (1997) 5383.
[5] T. Ziegler, Chem. Rev. 91 (1991) 651.
[6] J.H. MacNeil, A.C. Chiverton, S. Fortier, M.C. Baird, R.C. Hynes, A.J. Williams, K.F. Preston, T. Ziegler, J. Am. Chem. Soc. 113 (1991) 9834.
[7] L. Fan, T. Ziegler, J. Chem. Phys. 95 (1991) 7401.
[8] L. Fan, T. Ziegler, J. Phys. Chem. 96 (1992) 6937.
[9] R. Szilagyi, G. Frenking, Organometallics 16 (1997) 4807.
[10] A. Berces, T. Ziegler, L. Fan, J. Phys. Chem. 98 (1994) 1584.
[11] A. Berces, T. Ziegler, J. Phys. Chem. 98 (1994) 13233.
[12] A. Berces, T. Ziegler, J. Phys. Chem. 99 (1995) 11417.
[13] A. Berces, J. Phys. Chem. 100 (1996) 16538–16544.
[14] V. Jonas, W. Thiel, J. Chem. Phys. 102 (1995) 8474.
[15] V. Jonas, W. Thiel, J. Chem. Phys. 105 (1996) 3636.
[16] V. Jonas, W. Thiel, Organometallics 17 (1998) 353.
[17] K.G. Spears, J. Phys. Chem. A 101 (1997) 6273.
[18] C. Sosa, J. Andzelm, B. Elkin, E. Wimmer, K.D. Dobbs, D.A. Dixon, J. Phys. Chem. 96 (1992) 6630.
[19] V. Jonas, W. Thiel, J. Phys. Chem. A 103 (1999) 1381.
[20] C. Pollak, A. Rosa, E.J. Baerends, J. Am. Chem. Soc. 119 (1997) 7324.
[21] T. Ziegler, L. Cavallo, A. Berces, Organometallics 12 (1993) 3586.
[22] J. Li, G. Schreckenbach, T. Ziegler, J. Phys. Chem. 98 (1994) 4838.
[23] E.J. Weitz, J. Phys. Chem. 98 (1994) 11256.
[24] T. Ziegler, V. Tschinke, L. Fan, A.D. Becke, J. Am. Chem. Soc. 111 (1989) 9177.
[25] W.H. Wang, E. Weitz, J. Phys. Chem. A 101 (1997) 2358.
[26] J. Li, G. Schreckenbach, T. Ziegler, J. Am. Chem. Soc. 117 (1995) 486.
[27] M.C. Heitz, C. Daniel, J. Am. Chem. Soc. 119 (1997) 8269.
[28] O. Gonzalez-Blanco, V. Branchadell, J. Chem. Phys. 110 (1999) 778.
[29] S.A. Decker, M. Klobukowski, J. Am. Chem. Soc. 120 (1998) 9342.
[30] B. Delley, M. Wrinn, H.P. Luthi, J. Chem. Phys. 100 (1994) 5785.

[31] A.W. Ehlers, Y. Ruiz-Morales, E.J. Baerends, T. Ziegler, Inorg. Chem. 36 (1997) 5031.
[32] A. Rosa, E.J. Baerends, New J. Chem. 15 (1991) 815.
[33] E. Folga, T. Ziegler, J. Am. Chem. Soc. 115 (1993) 5169.
[34] A. Rosa, G. Ricciardi, E.J. Baerends, D.J. Stufkens, Inorg. Chem. 34 (1995) 3425.
[35] A. Rosa, A.W. Ehlers, E.J. Baerends, J.G. Snijders, G. te Velde, J. Phys. Chem. 100 (1996) 5690.
[36] A. Rosa, G. Ricciardi, E.J. Baerends, D.J. Stufkens, Inorg. Chem. 35 (1996) 2886.
[37] H. Jacobsen, T. Ziegler, J. Am. Chem. Soc. 118 (1996) 4631.
[38] F.A. Cotton, X. Feng, J. Am. Chem. Soc. 119 (1997) 7514.
[39] F.A. Cotton, X. Feng, J. Am. Chem. Soc. 120 (1998) 3387.
[40] S.A. Decker, O. Donini, M. Klobukowski, J. Phys. Chem. 101 (1997) 8734.
[41] T.A. Barckholtz, B.E. Bursten, in preparation.
[42] T.A. Barckholtz, B.E. Bursten, J. Am. Chem. Soc. 120 (1998) 1926.
[43] T.A. Barckholtz, B.E. Bursten, in preparation.
[44] M. Vitale, M.E. Archer, B.E. Bursten, Chem. Commun. (Cambridge) (1998) 179.
[45] J.A.M. Simoes, J.L. Beauchamp, Chem. Rev. 90 (1990) 629.
[46] T.J. Marks, ACS Symposium Series, vol. 428, American Chemical Society, Washington, DC, 1990.
[47] E.J. Baerends, P. Ros, Chem. Phys. 2 (1973) 52.
[48] E.J. Baerends, D.E. Ellis, P. Ros, Chem. Phys. 2 (1973) 41.
[49] G. te Velde, E.J. Baerends, J. Comp. Phys. 99 (1992) 84.
[50] S.H. Vosko, L. Wilk, M. Nusair, Can. J. Phys. 58 (1980) 1200.
[51] A.D. Becke, Phys. Rev. A 38 (1988) 3098.
[52] J.P. Perdew, Phys. Rev. B 33 (1986) 8822.
[53] C. Daniel, M. Benard, A. Dedieu, R. Wiest, A. Veillard, J. Phys. Chem. 88 (1984) 4805.
[54] C. Daniel, J. Phys. Chem. 95 (1991) 2394.
[55] P.D. Lyne, D.M.P. Mingos, T. Ziegler, A.J. Downs, Inorg. Chem. 32 (1993) 4785.
[56] C. Daniel, I. Hyla-Kryspin, J. Demuynck, A. Veillard, Nouv. J. Chim. 9 (1985) 581.
[57] H. Ryeng, O. Gropen, O. Swang, J. Phys. Chem. A 101 (1997) 8956.
[58] R.N. Perutz, J.J. Turner, Inorg. Chem. 14 (1975) 262.
[59] S.P. Church, M. Poliakoff, J.A. Timney, J.J. Turner, J. Am. Chem. Soc. 103 (1981) 7515.
[60] M. Poliakoff, J.J. Turner, J. Chem. Soc. Dalton Trans. (1974) 2276.
[61] L.A. Hanlan, H. Huber, E.P. Kundig, B.R. McGarvey, G.A. Ozin, J. Am. Chem. Soc. 97 (1975) 7054.
[62] K.P. Huber, G. Herzberg, Molecular spectra and molecular structure, in: Constants of Diatomic Molecules, vol. IV, Van Nostrand Reinhold, New York, 1979.
[63] J.A.M. Simoes, J.C. Schultz, J.L. Beauchamp, Organometallics 4 (1985) 1238.
[64] J.L. Goodman, K.S. Peters, V. Vaida, Organometallics 5 (1986) 815.
[65] A.F. Hepp, M.S. Wrighton, J. Am. Chem. Soc. 105 (1983) 5934.
[66] I.R. Dunkin, P. Harter, C.J. Shields, J. Am. Chem. Soc. 106 (1984) 7248.
[67] F.A. Kvietok, B.E. Bursten, Organometallics 14 (1995) 2395.
[68] J.A. Connor, Top. Curr. Chem. 71 (1977) 71.
[69] A.K. Baev, Russ. J. Phys. Chem. 54 (1980) 1.
[70] F.A. Cotton, Prog. Inorg. Chem. 21 (1976) 1.
[71] G. Bor, L. Noack, J. Organomet. Chem. 64 (1974) 367.
[72] G. Bor, Spectrochim. Acta 19 (1963) 2065.
[73] K. Noack, Spectrochim. Acta 19 (1963) 1925.
[74] K. Noack, Helv. Chim. Acta 47 (1964) 1064.
[75] K. Noack, Helv. Chim. Acta 47 (1964) 165.
[76] B.E. Hanson, M.J. Sullivan, R.J. Davis, J. Am. Chem. Soc. 106 (1984) 251.
[77] S. Goebel, C.L. Haynes, F.A. Khan, P.B. Armentrout, J. Am. Chem. Soc. 117 (1995) 6994.
[78] G. Pilcher, H.A. Skinner, in: F.R. Hartley, S. Patai (Eds.), The Chemistry of the Metal–Carbon Bond, vol. 1, Wiley, Chichester, 1982, pp. 43–90.
[79] D.R. Bidinosti, N.S. McIntyre, J. Chem. Soc. Chem. Commun. (1967) 1.
[80] D.R. Bidinosti, N.S. McIntyre, Can. J. Chem. 48 (1970) 593.
[81] R.J. Klingler, J.W. Rathke, J. Am. Chem. Soc. 116 (1994) 4772.
[82] G.P. Smith, Polyhedron 7 (1988) 1605.
[83] A.D. Becke, J. Chem. Phys. 96 (1992) 2155.
[84] A.D. Becke, J. Chem. Phys. 97 (1992) 9173.
[85] A.D. Becke, J. Chem. Phys. 98 (1993) 5648.
[86] A.D. Becke, J. Chem. Phys. 104 (1996) 1040.
[87] A.D. Becke, J. Chem. Phys. 107 (1997) 8554.
[88] K. Nakamoto, Infrared and Raman Spectra of Inorganic and Coordination Compounds, Wiley, New York, 1986.